Springer

Dear Author,

Here are the proofs of your article.

- You can submit your corrections **online**, via **e-mail** or by **fax**.
- For **online** submission please insert your corrections in the online correction form. Always indicate the line number to which the correction refers.
- You can also insert your corrections in the proof PDF and **email** the annotated PDF.
- For fax submission, please ensure that your corrections are clearly legible. Use a fine black pen and write the correction in the margin, not too close to the edge of the page.
- Remember to note the **journal title**, **article number**, and **your name** when sending your response via e-mail or fax.
- **Check** the metadata sheet to make sure that the header information, especially author names and the corresponding affiliations are correctly shown.
- **Check** the questions that may have arisen during copy editing and insert your answers/ corrections.
- **Check** that the text is complete and that all figures, tables and their legends are included. Also check the accuracy of special characters, equations, and electronic supplementary material if applicable. If necessary refer to the *Edited manuscript*.
- The publication of inaccurate data such as dosages and units can have serious consequences. Please take particular care that all such details are correct.
- Please **do not** make changes that involve only matters of style. We have generally introduced forms that follow the journal's style.
  Substantial changes in content, e.g., new results, corrected values, title and authorship are not allowed without the approval of the responsible editor. In such a case, please contact the Editorial Office and return his/her consent together with the proof.
- If we do not receive your corrections **within 48 hours**, we will send you a reminder.
- Your article will be published **Online First** approximately one week after receipt of your corrected proofs. This is the **official first publication** citable with the DOI. **Further changes are, therefore, not possible.**
- The **printed version** will follow in a forthcoming issue.

Please note

After online publication, subscribers (personal/institutional) to this journal will have access to the complete article via the DOI using the URL: http://dx.doi.org/[DOI].
If you would like to know when your article has been published online, take advantage of our free alert service. For registration and further information go to: http://www.link.springer.com.

Due to the electronic nature of the procedure, the manuscript and the original figures will only be returned to you on special request. When you return your corrections, please inform us if you would like to have these documents returned.

Metadata of the article that will be visualized in OnlineFirst

ArticleTitle	Validation of Fire Models Applied to Nuclear Power Plant Safety	
Article Sub-Title		
Article CopyRight	Springer Science+Business Media New York (Outside USA) (This will be the copyright line in the final PDF)	
Journal Name	Fire Technology	
Corresponding Author	Family Name	**McGrattan**
	Particle	
	Given Name	**Kevin**
	Suffix	
	Division	Fire Research Division
	Organization	National Institute of Standards and Technology
	Address	Gaithersburg, USA
	Email	kevin.mcgrattan@nist.gov
Author	Family Name	**Peacock**
	Particle	
	Given Name	**Richard**
	Suffix	
	Division	Fire Research Division
	Organization	National Institute of Standards and Technology
	Address	Gaithersburg, USA
	Email	
Author	Family Name	**Overholt**
	Particle	
	Given Name	**Kristopher**
	Suffix	
	Division	Fire Research Division
	Organization	National Institute of Standards and Technology
	Address	Gaithersburg, USA
	Email	

	Received	26 July 2014
Schedule	Revised	
	Accepted	4 October 2014

Abstract

The paper highlights key components of a fire model validation study conducted by the U.S. Nuclear Regulatory Commission and the Electric Power Research Institute. These include the selection of fire phenomena of interest to nuclear power plant safety, the selection of appropriate models, the selection of relevant experimental data, and the selection of appropriate evaluation criteria. For each model and each quantity of interest, there are two metrics of accuracy. The first is a bias factor, which indicates the extent to which the model tends to over or under-predict the given quantity. The second is a relative standard deviation, which indicates the degree of scatter in the predicted quantity when compared with experimental measurements. While the study is motivated by nuclear power plant safety, the general procedure and results are appropriate for most industrial applications.

Keywords (separated by '-') Fire modeling - Model validation - Nuclear power plants

Footnote Information

Fire Technology

DOI: 10.1007/s10694-014-0436-z

Validation of Fire Models Applied to Nuclear Power Plant Safety

Kevin McGrattan, Richard Peacock and Kristopher Overholt, Fire Research Division, National Institute of Standards and Technology, Gaithersburg, MD, USA*

Received: 26 July 2014/**Accepted:** 4 October 2014

Abstract. The paper highlights key components of a fire model validation study conducted by the U.S. Nuclear Regulatory Commission and the Electric Power Research Institute. These include the selection of fire phenomena of interest to nuclear power plant safety, the selection of appropriate models, the selection of relevant experimental data, and the selection of appropriate evaluation criteria. For each model and each quantity of interest, there are two metrics of accuracy. The first is a bias factor, which indicates the extent to which the model tends to over or under-predict the given quantity. The second is a relative standard deviation, which indicates the degree of scatter in the predicted quantity when compared with experimental measurements. While the study is motivated by nuclear power plant safety, the general procedure and results are appropriate for most industrial applications.

Keywords: Fire modeling, Model validation, Nuclear power plants

1. Introduction

Both domestically and worldwide, risk-informed and performance-based analyses are being introduced into fire protection engineering practice. One key tool needed to support performance-based design in fire protection is the availability of verified and validated fire models that can reliably predict the consequences of fires. Code requirements from the National Fire Protection Association (NFPA), and the International Code Council (ICC) acknowledge the need to understand the limitations of computer models applied to building design. NFPA 5000 [1] requires that the methods used to judge performance be shown to be valid and appropriate for the proposed use, including the impact of uncertainty on design calculations. NFPA 805 [2] includes provisions for models to be verified and validated for application to nuclear power plants. As part of a larger effort to support risk-informed design for nuclear power plants, the U.S. Nuclear Regulatory Commission (NRC) in cooperation with the Electrical Power Research Institute (EPRI) have published the results of an extensive validation effort for a range of fire calculation tools that may be used in power plant design [3]. This NRC/EPRI study, originally published in 2007 and updated in 2014, includes an evaluation of a selection of available fire models ranging from spreadsheet-based empirical

* Correspondence should be addressed to: Kevin McGrattan, E-mail: kevin.mcgrattan@nist.gov

correlations to a computational fluid dynamics (CFD) model. This paper includes a sampling of results of the empirical correlations, the Consolidated Fire and Smoke Transport zone fire model (CFAST), and the Fire Dynamics Simulator (FDS) CFD model. Included is a review of the experiments used in the comparisons with the models, an analysis of the uncertainty of the experiments, and a selection of quantitative comparisons of the model predictions with a range of experimental results that demonstrate the strengths and weaknesses of the models.

Given the complexity and range of features in current fire models, it is impractical to evaluate the accuracy of every model output. Thus, the study focuses on fire phenomena and hazards that are directly relevant for a range of compartment fire scenarios, such as the movement of smoke and hot gases from compartment to compartment, the integrity of electrical cables and fire barriers, and the effectiveness of smoke removal systems. Overall, 14 predicted quantities were chosen, including the depth and average temperature of the hot gas layer (HGL), ceiling jet and plume temperatures, radiant and total heat flux onto walls and "targets," and concentrations of combustion gas species and smoke.

2. Models and Predicted Quantities

The Office of Research of the U.S. Nuclear Regulatory Commission developed a set of spreadsheets to calculate commonly used empirical correlations of fire phenomena [4]. Table 1 lists the most widely used of the correlations.

CFAST [14] is a two-zone fire model that predicts the environment that arises within compartments as a result of a fire prescribed by the user. CFAST was developed and is maintained primarily by the Fire Research Division of NIST. CFAST calculates the average temperatures of the upper and lower gas layers within each compartment; layer interface position within each compartment; flame height; ceiling, wall, and floor temperatures within each compartment; flow

Table 1
List of Empirical Correlations Evaluated in the Study

Output quantity	Correlation
HGL temperature, natural ventilation	McCaffrey, Quintiere, Harkleroad (MQH) [5]
HGL temperature, forced ventilation	Foote, Pagni Alvares (FPA) [5]
	Deal and Beyler (DB) [5]
HGL temperature, no ventilation	Beyler [5]
Plume temperature	Heskestad [6]
	McCaffrey [7]
Ceiling jet temperature	Alpert [8]
Radiation heat flux	Point source method [9]
	Solid flame method [9]
Electrical cable failure time	Thermally-Induced Elec. Failure (THIEF) [10]
Steel temperature	Thermally-thin assumption [11]
Sprinkler activation time	DETACT [12]
Detector activation time	Temperature rise assumption [13]

through vents and openings; visible smoke and gas species concentrations within each layer; target temperatures; heat transfer to targets; sprinkler activation time; and the impact of sprinklers on the heat release rate (HRR) of the fire. CFAST version 6.3.1 was used in the study.

FDS [15] is a CFD model of fire-driven fluid flow. The model numerically solves a form of the Navier−Stokes equations appropriate for low-speed, thermally-driven flow, with an emphasis on smoke and heat transport from fires. The partial derivatives of the equations for conservation of mass, momentum, and energy are approximated as finite differences, and the solution is updated in time on a three-dimensional, rectilinear grid. Thermal radiation is computed using a finite volume technique on the same grid as the flow solver. Lagrangian particles are used to simulate smoke movement and sprinkler discharge. FDS computes the temperature, density, pressure, velocity, and chemical composition within each numerical grid cell at each discrete time step. There are typically hundreds of thousands to several million-grid cells, and thousands to hundreds of thousands of time steps. In addition, FDS computes the temperature, heat flux, mass loss rate, and various other quantities at solid surfaces. FDS version 6.0.0 was used in the study.

ASTM E1355 [16] provides guidance for evaluation of deterministic fire models for specific applications of interest. Following ASTM E1355, the organization(s) performing the validation study select the types of experiments and the measured quantities against which to compare the model predictions. In the case of the NRC/EPRI study, the following predicted quantities were judged to be of most relevance to nuclear power plant (NPP) safety:

Hot gas layer (HGL) temperature: The HGL temperature is particularly important for NPP fire scenarios because it is an indicator of overhead target damage (e.g., cable trays) away from the ignition source.

Hot gas layer depth: The depth of the HGL is important because it indicates whether a given target is immersed in high temperature gases.

Ceiling jet temperature: The ceiling jet is the shallow layer of hot gases that spreads radially below the ceiling as the fire plume impinges on it. The temperature of this layer is distinctly higher than the temperature associated with the HGL. The ceiling jet temperature is important in NPP fire scenarios where targets may be located just below the ceiling and for determining activation of heat detection devices.

Plume temperature: The fire plume is the buoyant flow of hot gases rising from the base of the fire. The fire plume transports hot gases into the HGL. Its temperature is greater than the ceiling jet and HGL temperature. It is particularly important in NPP fires because of the numerous postulated scenarios that involve targets directly above a potential fire.

Heat flux to targets: In NPP fire model analyses, damage to targets is assumed when either the surface temperature or heat flux exceeds specified limits. A target can be any object whose functionality of is importance to plant safety.

Surface (walls, floors, and ceilings) heat flux: Surface heat flux refers to the incident or net heat fluxes received by room surfaces such as walls, floors, or ceilings. This category of heat flux is considered separately from target heat flux to determine if the models have any particular strengths or weaknesses in their handling of walls, floors, and ceilings as opposed to objects within the compartment such as electrical cables.

Target temperature: Target temperature refers to the surface temperature of specific items within the computational domain. The calculation of the temperature of targets, e.g., electrical cables, is perhaps the most common objective of fire modeling analyses.

Cable failure time: Electrical cable failure time is often compared with the time to start detection and suppression activities. It specifically refers to the time it takes a fire to increase the surface or internal temperature of a cable to its damage or ignition temperature.

Surface (wall, floor and ceiling) temperature: As with heat flux, surface temperature of walls is distinguished from that of targets to determine if the models have particular strengths or weaknesses.

Smoke concentration: The smoke concentration can be an important quantity in NPP fire scenarios that involve rooms where operators may need to perform actions during a fire or where smoke detectors are installed.

Oxygen concentration: Oxygen concentration is an indicator of a fire becoming under-ventilated, which can be a pre-cursor to flashover.

Sprinkler activation time: Activation time of sprinklers or heat detectors is an important fire modeling output as it is often compared with the cable or target damage time. It specifically refers to the time it takes a fire to increase the temperature of the fusible link in a sprinkler or heat detection device.

Smoke detector activation time: Smoke detector activation time often serves as the trigger for suppression activities either by automatic systems or a fire brigade. It specifically refers to the time it takes a fire to generate the smoke concentration conditions sufficient to activate the smoke detection device.

Room pressure: Room pressure is a rarely used quantity in NPP fire modeling. It can be important if it affects smoke migration to adjacent compartments or the operation of mechanical ventilation.

3. Experiments and Experimental Uncertainty

This section includes a summary of the experiments used in the validation study, presents a review of the experimental uncertainty associated with these experiments for the measured quantities of interest, and discusses the range of the experimental data in terms of common parameters used in fire protection engineering.

3.1. Description of Experiments

Following is a list of experiments selected by the NRC and EPRI for the validation study. The criteria for selection included (1) the data are publicly available, (2) the experiments are well-documented, and (3) the fire scenarios are similar to what would be expected in an NPP.

ATF Corridor Experiments: A series of 18 experiments (six sets of three replicates) were conducted in a two-story structure with long hallways and a connecting stairway at the Alcohol, Tobacco, Firearms and Explosives (ATF) Fire Research Laboratory in Ammendale, Maryland, in 2008 [17]. The fuel source was a 0.4 m square natural gas burner.

Cable Response to Live Fire – CAROLFIRE: An experimental and modeling study sponsored by the NRC to study the thermal response and functional behavior of electrical cables [10]. The primary objective of CAROLFIRE was to characterize the various modes of electrical failure (e.g., hot shorts, shorts to ground) within bundles of power, control and instrument cables exposed to radiant heating and open fire sources. A secondary objective of the project was to develop a simple model to predict thermally-induced electrical failure (THIEF). The measurements used for these purposes were conducted at Sandia National Laboratories and are described in Vol. 2 of the CAROLFIRE test report. The modeling was conducted by NIST and documented in Vol. 3.

Fleury Heat Flux Measurements: Rob Fleury, a student at the University of Canterbury in Christchurch, New Zealand, measured the heat flux from one, two, or three adjacent 0.3 m square propane burners [18].

FM/SNL Experiments: The Factory Mutual and Sandia National Laboratories experiments consisted of 25 fire tests conducted in 1985 for the NRC by Factory Mutual Research Corporation (FMRC), under the direction of Sandia National Laboratories (SNL) [19, 20]. The primary purpose of these experiments was to provide data with which to validate computer models for various types of NPP compartments. The fires ranged from 0.9 m diameter propene burners to comparably sized pans of heptane.

iBMB Experiments: Several validation experiments were conducted at the Institut für Baustoffe, Massivbau und Brandschutz (iBMB) of the Braunschweig University of Technology in Germany as part of an international fire model validation program [3]. The tests were intended to study large pool fires in relatively small compartments. The fires were fueled by jet fuel and ethanol in pans ranging in diameter from 0.5 m to 1.0 m.

LLNL Enclosure Experiments: Sixty-four experiments were conducted by Lawrence Livermore National Laboratory (LLNL) in 1986 to study the effects of ventilation on enclosure fires [21]. The fires were fueled by a 0.6 m diameter natural gas burner.

NBS Multi-Compartment Experiments: The National Bureau of Standards (NBS, which is now called the National Institute of Standards and Technology, NIST) Multi-Compartment Test Series consisted of 45 fire tests representing 9 different sets of conditions were conducted in a three-room suite in 1985 [22]. The suite consisted of two relatively small rooms, connected via a relatively long corridor. The fire source, a 0.3 m square natural gas burner, was located against the rear wall of one of the small compartments.

NIST/NRC Compartment Experiments: A series of 15 large-scale experiments sponsored by NRC and performed at NIST in 2003 [23]. The fire sizes ranged from 350 kW to 2.3 MW in a compartment designed to resemble a switchgear room in an NPP. The fire was fueled with either heptane or toluene sprayed into a 0.5 m by 1.0 m rectangular pan.

NIST Smoke Alarm Experiments: A series of experiments was conducted by NIST to measure the activation time of ionization and photoelectric smoke alarms in a residential setting [24]. Tests were conducted in actual homes with representative sizes and floor plans, utilized actual furnishings and household items for fire sources, and tested actual smoke alarms commercially available at that time.

SP Adiabatic Surface Temperature Experiments: In 2008, three compartment experiments were performed at SP Technical Research Institute of Sweden under the sponsorship of Brandforsk, the Swedish Fire Research Board [25]. The fires were fueled by a 0.3 m square natural gas burner. The objective of the experiments was to demonstrate how plate thermometer measurements in the vicinity of a simple steel beam can be used to supply the boundary conditions for a multi-dimensional heat conduction calculation for the beam.

Steckler Compartment Experiments: Steckler, Quintiere and Rinkinen performed a set of 55 compartment fire tests at NBS in 1979 [26]. The compartment was 2.8 m by 2.8 m by 2.13 m high, with a single door of various widths, or alternatively a single window with various heights. The fires were fueled by a 0.3 m diameter natural gas burner. The tests were conducted to study entrainment and vent flow induced by a compartment fire.

UL/NIST Vent Experiments: In 2012, the Fire Fighting Technology Group at NIST conducted experiments at Underwriters Laboratories (UL) in Northbrook, Illinois, to assess the change in compartment temperature due to the opening of one or two 1.2 m square ceiling vents [27]. The fires were fueled by a 0.8 m square natural gas burner.

UL/NFPRF Sprinkler, Vent, and Draft Curtain Experiments: In 1997, a series of 34 heptane spray burner experiments was conducted at the Large Scale Fire Test Facility at Underwriters Laboratories (UL) in Northbrook, Illinois [28, 29]. The experiments were divided into two test series. Series I consisted of twenty-two 4.4 MW fire experiments. Series II consisted of twelve 10 MW fire experiments. The objective of the experiments was to characterize the temperature and flow field for fire scenarios with a controlled heat release rate in the presence of sprinklers, draft curtains, and smoke and heat vents.

U.S. Navy High Bay Hangar Experiments: The U.S. Navy (USN) sponsored a series of 33 experiments within two hangars examining fire detection and sprinkler activation in response to spill fires in large enclosures. Experiments were conducted using JP-5 and JP-8 fuels in two Navy high bay aircraft hangars located in Naval Air Stations in Barbers Point, Hawaii and Keflavik, Iceland [30]. Eleven experiments were conducted in Hawaii, twenty-two in Iceland.

Vettori Ceiling Sprinkler Experiments: Robert Vettori analyzed a series of 45 experiments conducted at NIST that were intended to compare the effects of different ceiling configurations on the activation times of quick response residential pendent sprinklers. The test parameters consisted of two ceiling configurations, three fire growth rates, and three burner locations a total of 18 unique test configurations with sets of two or three replicates each [31]. The 0.7 m by 1.0 m burner was fueled by natural gas. Vettori analyzed a similar set of sprinkler experiments involving ceilings of various slopes [32].

VTT Large Experiments: The VTT large hall tests consisted of eight heptane pan fire experiments conducted in 1998 and 1999 [33]. The experiments represented three sets of conditions, and were undertaken to study the movement of smoke in a large hall with a sloped ceiling. The results of the experiments were contributed to the International Collaborative Fire Model Project (ICFMP) for use in evaluating model predictions of fires in large volumes representative of turbine halls in NPPs.

WTC Spray Burner Experiments: As part of its investigation of the World Trade Center (WTC) disaster, the Building and Fire Research Laboratory at NIST conducted several series of fire experiments to both gain insight into the observed fire behavior and also to validate FDS for use in reconstructing the fires. The first series of experiments involved a relatively simple compartment with a liquid spray heptane/toluene burner and various structural elements with varying amounts of sprayed fire-resistive materials [34].

3.2. Experimental Uncertainty

With a few exceptions, the test reports for the experiments described above contain little information about the experimental uncertainty. However, the report by Hamins et al. of the NIST/NRC Experiments [23] contains a fairly extensive discussion of the uncertainties of measurement devices that were used in the experiments chosen for the study. Using this information, estimates of experimental uncertainty were made for all the experiments as a whole. Details can be found in Ref. [3].

Table 2 summarizes the estimated uncertainties of the measurements of the quantities of interest. The *Measurement Uncertainty* refers to the measurement device itself, such as a thermocouple, heat flux gauge, etc. The *Propagated Input Uncertainty* refers to the uncertainty in the quantity of interest that is associated with the uncertainty of key measured input parameters, such as the heat release rate or ventilation rate. For example, the propagated input uncertainty of the predicted gas and solid temperatures, 0.05, is largely due to the uncertainty in the heat release rate, which has been estimated to be approximately 0.075. Various hot gas layer and plume correlations (like MQH) predict that the temperature rise is proportional to the heat release rate raised to the two-thirds power. Therefore, the propagated uncertainty in the temperature predictions is expected to be two-thirds of the uncertainty in the heat release rate.

The *Combined Uncertainty* represents the total experimental uncertainty, denoted as $\widetilde{\sigma}_E$, is obtained by taking the square root of the sum of the squares of the measurement and parameter propagation uncertainties.

3.3. Summary of Experimental Parameters

Table 3 presents a summary of the experiments in terms of parameters commonly used in fire protection engineering. This "parameter space" outlines the range of applicability of the models included in the validation study. In other words, if this validation study is to be cited as justification for using a given model to simulate

Table 2
Summary of Uncertainty Estimates

Output quantity	Measurement Uncertainty	Propagated Input Uncertainty	Combined Uncertainty, $\widetilde{\sigma}_E$
Gas and solid temperatures	0.05	0.05	0.07
HGL depth	0.05	0.00	0.05
Gas concentrations	0.02	0.08	0.08
Smoke concentration	0.14	0.13	0.19
Pressure, closed compartment	0.01	0.21	0.21
Pressure, open compartment	0.01	0.15	0.15
Velocity	0.07	0.03	0.08
Heat flux	0.05	0.10	0.11
No. activated sprinklers	0.00	0.15	0.15
Sprinkler activation time	0.00	0.06	0.06
Cable failure time	0.00	0.12	0.12
Smoke alarm activation time	0.00	0.34	0.34

All values are expressed in the form of a standard relative uncertainty

a given fire scenario, that scenario must be similar to these experiments in the sense of having comparable physical parameters. These parameters are explained below:

Fire Froude Number, $\dot{Q}^*$, is a useful non-dimensional quantity for plume correlations and flame height estimates:

$$\dot{Q}^* = \frac{\dot{Q}}{\rho_\infty c_p T_\infty \sqrt{gD} D^2} \tag{1}$$

Table 3
Summary of Important Experimental Parameters

Test series	$\dot{Q}^*$	L_f/H	ϕ	W/H	L/H	r_{cj}/H	r_{rad}/D
ATF	0.3–3.3	0.3–0.9	0.0–0.1	0.8	7.1	0.8–6.0	N/A
Fleury	0.3–5.5	Open	Open	Open	Open	Open	1.7–3.3
FM/SNL	0.6–2.4	0.3–0.6	0.0–0.2	2.0	3.0	0.2–0.3	N/A
LLNL	0.2–1.5	0.1–0.4	0.1–0.4	0.9	1.3	0.3–1.0	N/A
NBS	1.5	0.5	0.0	1.0	5.1	N/A	N/A
NIST/NRC	0.3–2.0	0.3–1.0	0.0–0.3	1.9	5.7	0.3–2.1	2.0–4.0
NIST Alarms	0.2–0.3	0.2–0.5	N/A	1.7	8.3	1.3–8.3	N/A
SP AST	6.1	1.1	0.1	1.0	1.5	N/A	N/A
Steckler	0.8–3.8	0.3–0.7	0.0–0.6	1.3	1.3	N/A	N/A
UL/NFPRF	4.0–9.1	0.7–1.0	Open	4.9	4.9	0.6–3.9	N/A
UL/NIST	0.7–2.6	0.8–1.6	0.2–0.6	1.8	2.5	1.0–2.3	N/A
USN Hawaii	0.7–1.3	0.1–0.4	Open	4.9	6.5	0–1.2	N/A
USN Iceland	0.7–1.3	0.0–0.3	Open	2.1	3.4	0–1.0	N/A
Vettori	2.5	1.1	0.3	2.1	3.5	0.8–2.9	N/A
VTT	0.7	0.2	0	1.0	1.4	0–0.6	N/A
WTC	0.6–0.9	0.8–1.1	0.3–0.5	0.9	1.8	0.0–0.8	0.3–1.3

where $\dot{Q}$ is the peak heat release rate of the fire, ρ_∞ is the ambient density, c_p is the specific heat of the air, T_∞ is the ambient temperature, g is the acceleration of gravity, and D is the equivalent diameter of the base of the fire, calculated as $D = \sqrt{4A/\pi}$, where A is the area of the base. $\dot{Q}^*$ is essentially the ratio of the fuel gas exit velocity and the buoyancy-induced plume velocity. Jet fires are characterized by large Froude numbers. Typical accidental fires have a Froude number near unity.

Flame Height Relative to Ceiling Height, L_f/H, is a convenient way to express the physical size of the fire relative to the height of the room, H. The height of the visible flame, based on Heskestad's correlation, is estimated by:

$$L_f = D\left(3.7\,(\dot{Q}^*)^{2/5} - 1.02\right) \tag{2}$$

Global Equivalence Ratio, ϕ, is the ratio of the mass flux of fuel, $\dot{m}_\mathrm{f}$, to the mass flux of oxygen, $\dot{m}_{\mathrm{O}_2}$, into the compartment divided by the stoichiometric ratio, r.

$$\phi = \frac{\dot{m}_\mathrm{f}}{r\,\dot{m}_{\mathrm{O}_2}} \equiv \frac{\dot{Q}\ (\mathrm{kW})}{13,100\ (\mathrm{kJ/kg})\ \dot{m}_{\mathrm{O}_2}} \tag{3}$$

The supply rate of oxygen to the compartment depends on whether it is naturally or mechanically ventilated:

$$\dot{m}_{\mathrm{O}_2} = \begin{cases} \frac{1}{2}\,0.23\,A_0\sqrt{H_0} & : \quad \text{Natural Ventilation} \\ 0.23\,\rho_\infty\,\dot{V} & : \quad \text{Mechanical Ventilation} \end{cases} \tag{4}$$

Here, A_0 is the area of the compartment opening, H_0 is the height of the opening, and $\dot{V}$ is the volume flow of air into the compartment. If $\phi < 1$, the compartment is considered "well-ventilated" and if $\phi > 1$, the compartment is considered "under-ventilated."

Compartment Aspect Ratios, W/H **and** L/H, where W and L represent the width and length, indicate if the compartment is shaped like a hallway, typical room, or vertical shaft.

Relative Distance along the Ceiling, r_cj/H, indicates the distance away from the fire plume centerline of a sprinkler, smoke detector, etc., relative to the compartment height, H. The subscript "cj" denotes ceiling jet.

Relative Distance from the Fire, r_rad/D, indicates whether a "target" is near or far from the fire. This ratio is of importance in a radiation calculation.

4. Model Uncertainty

The experiments described in the previous section involved thousands of individual point measurements of gas and surface temperatures, heat fluxes, gas concentrations, and so on. These measurements are typically made continuously during the experiment, and the models make predictions of these same quantities at the same sampling frequency. This leads to hundreds of thousands of point to point comparisons of model predictions and experimental measurements. These results must be reduced to a more tractable form. Peacock et al. [35] discuss various ways of comparing two time histories of a given quantity. A commonly used metric is simply to compare the measured and predicted peak values. If the data are spiky, some form of time-averaging can be used. Regardless of the exact form of the metric, what results from this exercise is a pair of numbers for each time history, (E_i, M_i), where i ranges from 1 to n and both M_i and E_i are positive numbers expressing the increase in the value of a quantity above its ambient. For a given quantity of interest, there might be hundreds of these pairs. These data need to be reduced even further so that one can evaluate the model uncertainty in predicting the given quantity. The basic idea is to express the accuracy of the models in predicting a given quantity of interest using a pair of statistics. The first is a bias factor, δ, which expresses the tendency of the model to over or under-predict the measured quantity. For example, a bias factor of 1.10 indicates that the model, on average, over-predicts the measured quantity by 10 %. The second statistic is a relative standard uncertainty that indicates the degree of scatter about the mean. How these values are used in practice will be described below. Details of the statistical analysis are described in detail in Ref. [36] and summarized here.

To estimate the mean and standard deviation of the distribution, first define:

$$\overline{\ln(M/E)} = \frac{1}{n}\sum_{i=1}^{n} \ln(M_i/E_i) \tag{5}$$

Note that the logarithm is used because the standard deviation of the logarithm of a normally distributed random variable is approximately equal to the standard deviation divided by the mean, the relative standard deviation.

The least squares estimate of the standard deviation of the combined distribution is defined as:

$$\widetilde{\sigma}_M^2 + \widetilde{\sigma}_E^2 = \frac{1}{n-1}\sum_{i=1}^{n}\left[\ln(M_i/E_i) - \overline{\ln(M/E)}\right]^2 \tag{6}$$

Recall that $\widetilde{\sigma}_E$ is known and the expression on the right can be evaluated using the pairs of measured and predicted values. Equation (6) imposes a constraint on the value of the experimental uncertainty, $\widetilde{\sigma}_E$. A further constraint is that $\widetilde{\sigma}_M$ cannot be less than $\widetilde{\sigma}_E$ because it is not possible to demonstrate that the model is more accurate than the measurements against which it is compared. Combining the two constraints leads to:

$$\widetilde{\sigma}_E^2 < \frac{1}{2}\mathrm{Var}(\ln(M/E)) \tag{7}$$

An estimate of δ can be found using the mean of the distribution:

$$\delta = \exp\left(\overline{\ln(M/E)} + \frac{\widetilde{\sigma}_M^2}{2} - \frac{\widetilde{\sigma}_E^2}{2}\right) \tag{8}$$

For a given model prediction, M, of the quantity of interest whose bias factor, δ, and relative standard deviation, $\widetilde{\sigma}_M$, have been calculated from all of the available validation data, the true (but unknown) value of this quantity, θ, is assumed to be normally distributed:

$$\theta \sim N\left(\frac{M}{\delta}\ ,\ \widetilde{\sigma}_M^2\left(\frac{M}{\delta}\right)^2\right) \tag{9}$$

The mean and variance of this normal distribution are based solely on comparisons of model predictions with past experiments that are similar to the particular fire scenario being analyzed. The performance of the model is quantified by the estimators of the parameters, δ and $\widetilde{\sigma}_M$, which have been corrected to account for uncertainties associated with the experimental measurements.

As an example of how to make use of Eq. (9), suppose a fire model is being used to estimate the likelihood that electrical control cables could be damaged due to a fire in a compartment. Damage is assumed to occur when the surface temperature of any cable reaches 200°C. What is the likelihood that the cables would be damaged if the model predicts that the maximum surface temperature of the cables is 175°C? First, consider for this example that the model bias factor, δ, is 1.13 and the relative standard deviation, $\widetilde{\sigma}_M$, is 0.20. Now, Consider the distribution, Eq. (9), of the "true" temperature, θ, shown graphically in Figure 1. The vertical lines indicate the critical temperature at which damage is assumed to occur ($T_c = 200$°C), and the temperature predicted by the model (175°C). Given an ambient temperature of 20°C, the predicted temperature rise, M, is 155°C. The mean and standard deviation in Eq. (9) are calculated:

$$\mu = 20 + \frac{M}{\delta} = 20 + \frac{155}{1.13} = 157°\text{C} \tag{10}$$

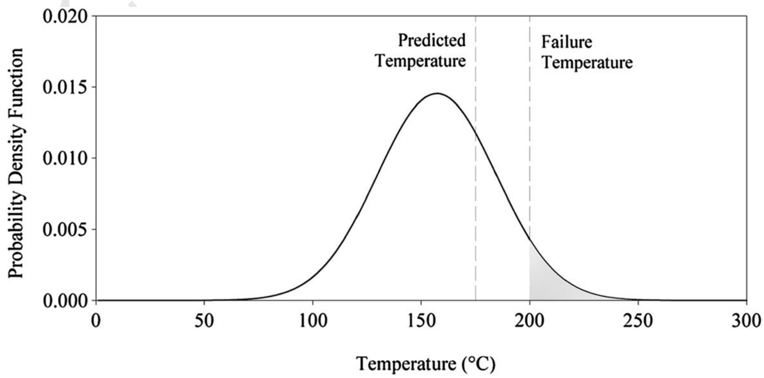

Figure 1. Plot showing a possible way of expressing the uncertainty of the model prediction.

$$\sigma = \widetilde{\sigma}_M \frac{M}{\delta} = 0.20 \times \frac{155}{1.13} = 27^{\circ}\mathrm{C} \tag{11}$$

respectively. The shaded area beneath the bell curve is the probability that the "true" temperature can exceed the critical value, $T_c = 200^{\circ}\mathrm{C}$, which can be expressed via the *complimentary error function*:

$$P(T > T_c) = \frac{1}{2}\mathrm{erfc}\left(\frac{T_c - \mu}{\sigma\sqrt{2}}\right) = \frac{1}{2}\mathrm{erfc}\left(\frac{200 - 157}{27\sqrt{2}}\right) \approx 0.06 \tag{12}$$

This means that there is a 6 % chance that the cables could become damaged, assuming that the model's input parameters are not subject to uncertainty.

5. Sample Results

This section presents a sample of results from the NRC/EPRI validation study [3]. The results of the full study are summarized in Table 4.

5.1. HGL Temperature

The empirical correlations and zone models predict an average HGL temperature, while CFD models predict the local gas temperature in each computational grid

Table 4
Model Uncertainty Metrics for All Quantities of Interest

	Empirical correlations			CFAST		FDS	
Output quantity	Name	δ	$\widetilde{\sigma}_M$	δ	$\widetilde{\sigma}_M$	δ	$\widetilde{\sigma}_M$
HGL temperature, natural	MQH	1.17	0.15	1.20	0.36	1.02	0.12
HGL temperature, forced	FPA	1.29	0.32				
	DB	1.18	0.25	1.15	0.19	1.21	0.22
HGL temperature, closed	Beyler	1.04	0.37	1.00	0.08	1.20	0.12
HGL depth	–	–	–	1.05	0.34	1.03	0.06
Ceiling jet temperature	Alpert	0.86	0.11	1.16	0.39	0.98	0.14
Plume temperature	Heskestad	0.84	0.33				
	McCaffrey	0.90	0.31	1.07	0.20	1.20	0.21
Oxygen concentration	–	–	–	1.00	0.15	1.01	0.11
Smoke concentration	–	–	–	3.69	0.68	2.63	0.59
Pressure rise	–	–	–	1.77	0.63	0.96	0.27
Target temperature	Steel	1.29	0.45	1.58	0.64	0.98	0.18
Target heat flux	Point source	1.44	0.47				
	Solid flame	1.17	0.44	0.97	1.16	0.98	0.25
Surface temperature	–	–	–	1.05	0.28	0.99	0.12
Surface heat flux	–	–	–	0.99	0.35	0.92	0.15
Cable failure time	THIEF	0.90	0.11	–	–	1.10	0.16
Sprinkler activation time	RTI	1.11	0.41	0.79	0.21	0.93	0.15
Detector activation time	Temp. rise	0.66	0.57	1.12	0.46	0.85	0.29

cell. For the purpose of comparing all of the models with experimental measurements, both the CFD predictions and experimental measurements of local gas temperatures can be spatially averaged to form a representative average HGL temperature. Because there are different empirical correlations governing compartments that are naturally ventilated, mechanically ventilated, or unventilated, the results for HGL temperature are divided into three categories; natural, forced and no ventilation. The natural ventilation results are discussed here. Natural ventilation refers to compartments with no mechanical ventilation system operational during the test and passive openings to the outside.

The results for the MQH correlation, CFAST, and FDS are shown in Figure 2. Note that the MQH correlation is only intended for a single compartment and vertical vents, and, thus, only includes a subset of the available experimental data. For the empirical correlations, the validation results do not include the UL/NIST Vents experiments (due to the presence of ceiling vents), the ATF Corridors experiments (due to the multi-story compartment configuration), or the VTT experiments (due to vents that were located high in the compartment, complex wall lining materials, and irregular geometry).

CFAST, the zone model, has simulated all of the experiments, and the increased scatter in its predictions compared to the empirical correlations are due to inclusion of additional experiments that the MQH correlation cannot address. The UL/NIST Vents experiments are noticeably over-predicted. These tests include large vents in the ceiling of the compartment that may extend beyond the original vent sizes of the empirical correlation used to determine flow through ceiling vents. In addition, the combination of larger HGL temperature and smaller HGL depth compared to the experimental data suggest that part of the difference may be attributed to the reduction method used to estimate layer temperature and position from the individual temperature measurements in the experiments.

There is no obvious bias in the FDS predictions, and no particular trends in the data. The relatively low bias and model relative standard deviation suggest that FDS HGL predictions are close to experimental uncertainty. FDS does not calculate an HGL temperature directly. Rather, it predicts the gas temperatures at the same locations as the experimental measurements, and the HGL temperature is calculated in the exact same way as it is for the experimental data.

5.2. Plume Temperature

There exist a variety of empirical correlations that predict the plume temperature, and these correlations are also embedded within the zone models. CFD models compute the plume temperature directly from the fundamental equations of motion. The results for the McCaffrey correlation, CFAST and FDS are shown in Figure 3. In this case, CFAST, the zone model, is the most accurate for two reasons. First, CFAST uses the McCaffrey correlation to calculate plume temperature and entrainment, but it includes the effect of the HGL. Second, FDS does not employ an empirical correlation and calculates the plume temperature directly from the governing equations. This is a possible explanation of the fact that CFAST has less of a bias in predicting plume temperature than FDS.

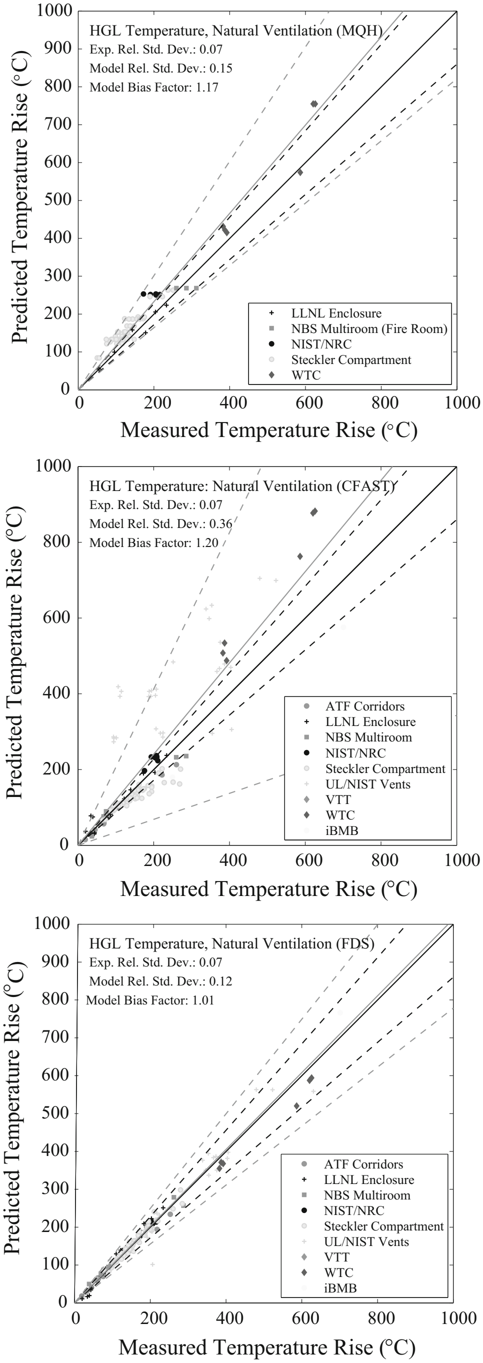

Figure 2. Summary of measured and predicted HGL temperatures under natural ventilation conditions.

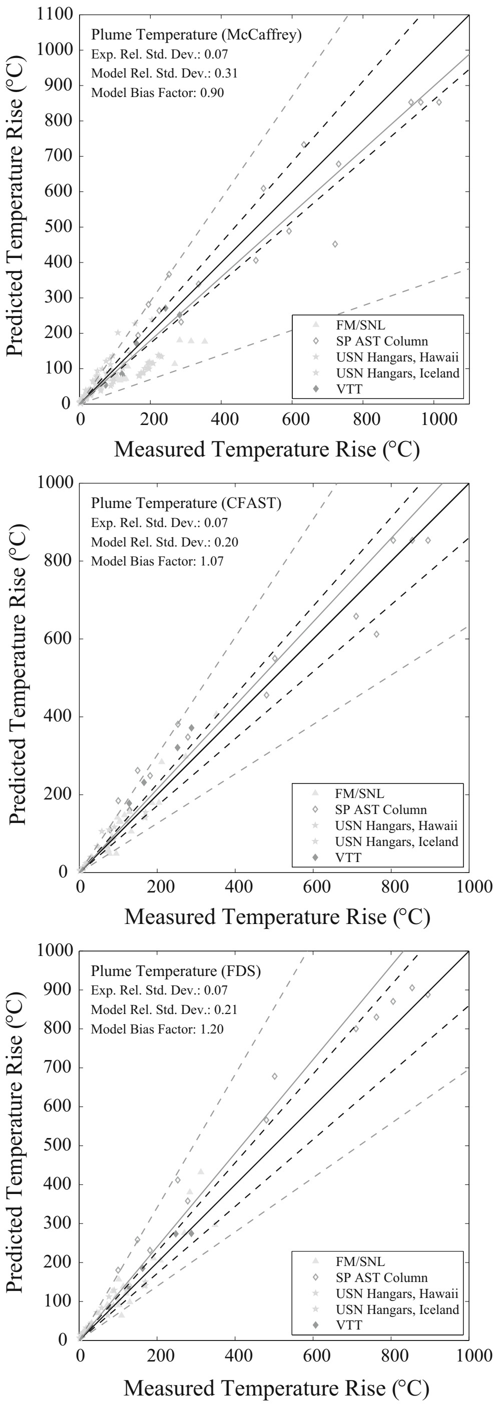

Figure 3. Summary of measured and predicted plume temperatures.

5.3. Target Temperature

The results for predicted target temperature are shown in Figure 4. The targets include unprotected and protected steel members and electrical cables. For the

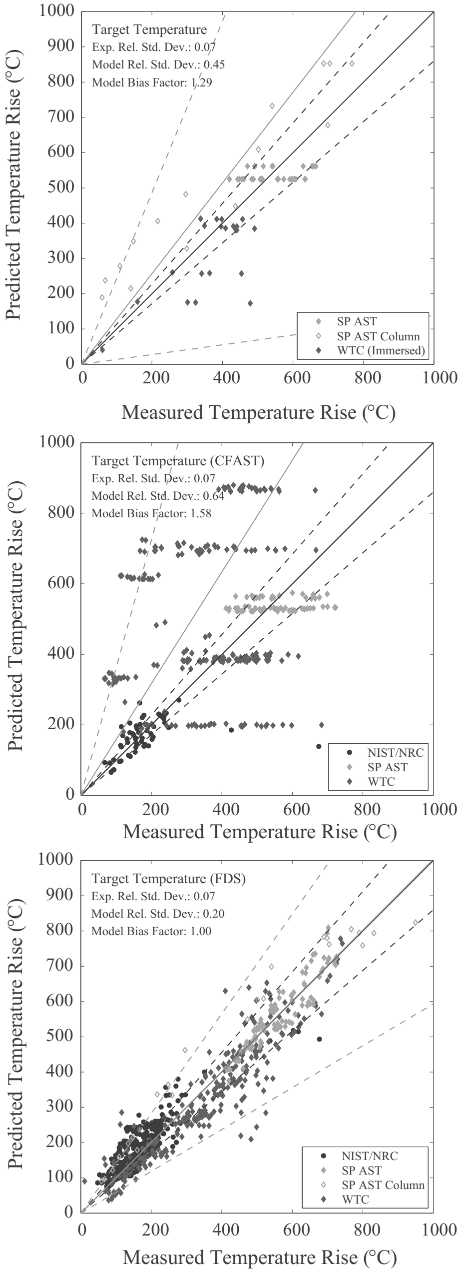

Figure 4. Summary of measured and predicted target temperatures.

empirical correlations, the exposing temperatures were provided by either the MQH HGL temperature correlation or the McCaffrey plume correlation, depending on the location of the target relative to the fire. The uncertainty in these predictions is often based on the selection of the exposing conditions, rather than the calculation of the target response. As with the correlations, the averaging of the HGL temperature in a zone model accounts for much of the uncertainty in its prediction of target response. Similar to the HGL temperature comparisons, the increased scatter in the CFAST predictions compared to the empirical correlations are likely due to inclusion of additional experiments that the correlations cannot address. In addition, for CFAST, the effects on target heating from the fire plume are only directly included if the target is located directly over the fire centerline. For targets near but off-center, only the impact of the average hot gas layer temperature is included. The FDS results show no obvious bias or trend.

5.4. Summary of All Quantities of Interest

Table 4 summarizes the results of the validation study. For each model and each quantity of interest, the model bias factor and relative standard deviation are listed. Note that the empirical correlations could not be applied to all of the quantities.

6. How to Use the Results of the Validation Study

The following steps outline the main components of a fire modeling analysis for nuclear power plant applications. With the exception of specific references to nuclear-specific guidance documents, this basic procedure can be applied to most any fire modeling study.

1. Postulate a fire scenario. NFPA 805 [2] provides guidance in selecting fire scenarios in NPP applications.
2. Choose an appropriate model. The summary scatter plots such as those shown above can help determine the level of accuracy expected of the various types of models.
3. For the given fire scenarios that are postulated as part of the overall analysis, the modeler must check that the parameters described in Sect. 3.3, applied to the postulated scenarios, are appropriate given the parameter space defined by the listed experiments. In other words, are the postulated fire scenarios within the range of validation of the chosen model?
4. All of the model results should be presented with an appropriate statement of model uncertainty. For NPP applications, the example in Sect. 4 is typical because most fire model calculations are performed to determine the likelihood that a given temperature or heat flux threshold is exceeded. This question can be answered directly in a way that incorporates the model uncertainty, e.g., there is a 6 % chance that the temperature of the cable will exceed 200°C.

These last two steps address common complaints by some in the fire community that models are used inappropriately and that models results cannot be trusted.

The remedy for this problem is to design the fire modeling process specifically to address these concerns. It is not sufficient for the modeler to simply claim that the chosen model is appropriate; he/she must prove it by citing relevant validation studies, demonstrating that the given application is within the model's range of validity, and quantifying the effect of model uncertainty on the model predictions. Model uncertainty analysis is no longer an option—it is an integral part of the process.

References

1. National Fire Protection Association (2012) Quincy, NFPA 5000: Building Construction and Safety Code
2. National Fire Protection Association (2001) Quincy, NFPA 805: Performance-based standard for fire protection for light-water reactor electric generating plants
3. Stroup D, Lindeman A (2013) Verification and validation of selected fire models for nuclear power plant applications. NUREG-1824, supplement 1, United States Nuclear Regulatory Commission, Washington, DC
4. Iqbal N, Salley M, Fire Dynamics Tools (FDTs): (2004) Quantitative fire hazard analysis methods for the U.S. Nuclear Regulatory Commission Fire Protection Inspection Program. NUREG-1805, United States Nuclear Regulatory Commission, Washington, DC
5. Walton W, Thomas P (2008) SFPE handbook of fire protection engineering. In: Estimating temperatures in compartment fires, 4th edn. National Fire Protection Association, Quincy
6. Heskestad G (2008) SFPE handbook of fire protection engineering. In: Fire plumes, flame height and air entrainment, 4th edn. National Fire Protection Association, Quincy
7. McCaffrey B (1979) Purely buoyant diffusion flames: some experimental results. NBSIR 79–1910, National Bureau of Standards (now NIST), Gaithersburg
8. Alpert R (2008) SFPE handbook of fire protection engineering. In: Ceiling jet flows, 4th edn. National Fire Protection Association, Quincy
9. Beyler C (2008) SFPE handbook of fire protection engineering. In: Flammability limits of premixed and diffusion flames, 4th edn. National Fire Protection Association, Quincy
10. Nowlen S, Wyant F, McGrattan K (2008) Cable response to live fire (CAROLFIRE). NUREG/CR 6931, United States Nuclear Regulatory Commission, Washington, DC
11. Mowrer F. (2008) SFPE handbook of fire protection engineering In: Enclosure smoke filling and fire-generated environmental conditions, 4th edn. National Fire Protection Association, Quincy
12. Evans D, Madrzykowski D (1981) Characterizing the thermal response of fusible-link sprinklers. NBSIR 81–2329, National Bureau of Standards (now NIST), Gaithersburg
13. Heskestad G, Delichatsios M (1977) Environments of fire detectors—Phase 1: Effects of fire size, ceiling height and material. Tech. Rep. NBS GCR 77–86 and NBS GCR 77–95, National Bureau of Standards (now NIST), Gaithersburg
14. Peacock RD, Forney GP, Reneke PA (2011) CFAST—Consolidated model of fire growth and smoke transport (Version 6): Technical Reference Guide. Special Publication 1026, National Institute of Standards and Technology, Gaithersburg

15. McGrattan K, Hostikka S, McDermott R, Floyd J, Weinschenk C, Overholt K (2013) Fire dynamics simulator, Technical Reference Guide. National Institute of Standards and Technology, Gaithersburg, and VTT Technical Research Centre of Finland, Espoo, 6th edn. Vol. 1: Mathematical Model; Vol. 2: Verification Guide; Vol. 3: Validation Guide; Vol. 4: Configuration Management Plan
16. American Society for Testing and Materials, West Conshohocken, Pennsylvania, ASTM E1355–12, Standard Guide for Evaluating the Predictive Capabilities of Deterministic Fire Models (2012)
17. Sheppard D, Klein B (2009) Burn tests in two story structure with hallways. Tech. rep, ATF Laboratories, Ammendale
18. Fleury R (2010) Evaluation of thermal radiation models for fire spread between objects. Master's thesis, University of Canterbury, Christchurch
19. Nowlen S (1987) Enclosure environment characterization testing for the baseline validation of computer fire simulation codes. NUREG/CR-4681 (SAND86-1296), Sandia National Laboratory, Albuqueque, New Mexico. Work performed under contract to the US Nuclear Regulatory Agency, Washington DC
20. Chavez J, Nowlen S (1988) An experimental investigation of internally ignited fires in nuclear power plant control cabinets, Part II: Room effects tests. NUREG/CR-4527 (SAND86-0336), Sandia National Laboratory, Albuqueque, New Mexico . Work performed under contract to the US Nuclear Regulatory Agency, Washington DC
21. Foote K (1987) 1986 LLNL Enclosure Fire Tests Data Report. Tech. Rep. UCID-21236, Lawrence Livermore National Laboratory
22. Peacock R, Davis S, Lee W (1988) An experimental sata set for the accuracy assessment of room fire models. NBSIR 88–3752, National Bureau of Standards (now NIST), Gaithersburg
23. Hamins A, Maranghides A, Johnsson R, Donnelly M, Yang G, Mulholland G, Anleitner R (2006) Report of Experimental Results for the International Fire Model Benchmarking and Validation Exercise 3. NIST Special Publication 1013–1, National Institute of Standards and Technology, Gaithersburg, Maryland . Joint Publication of NIST and the US Nuclear Regulatory Commission (NUREG/CR-6905)
24. Bukowski R, Peacock R, Averill J, Cleary T, Bryner N, Walton W, Reneke P, Kuligowski E (2008) Performance of home smoke alarms analysis of the response of several available technologies in residential fire settings. NIST Technical Note 1455–1, National Institute of Standards and Technology, Gaithersburg
25. Wickström U, Jansson R, Tuovinen H (2009) Verification fire tests on using the adiabatic surface temperature for predicting heat transfer. Tech. Rep. 2009:19, SP Technical Research Institute of Sweden, B0ras, Sweden
26. Steckler K, Quintiere J, Rinkinen W (1982) Flow induced by fire in a compartment. NBSIR 82–2520, National Bureau of Standards (now NIST), Gaithersburg
27. Opert K (2012) Assessment of natural vertical ventilation for smoke and hot gas layer control in a residential scale structure. Master's thesis, University of Maryland, College Park
28. Sheppard D, Steppan D (1997) Sprinkler, heat & smoke vent, draft curtain project—Phase 1 Scoping tests. Tech. rep. Underwriters Laboratories, Northbrook
29. McGrattan K, Hamins A, Stroup D (1988) Sprinkler, smoke & heat vent, draft curtain interaction—large scale experiments and model development. NISTIR 6196–1, National Institute of Standards and Technology, Gaithersburg
30. Gott J, Lowe D, Notarianni K, Davis W (1997) Analysis of high bay hangar facilities for fire detector sensitivity and placement. NIST Technical Note 1423, National Institute of Standards and Technology, Gaithersburg

31. Vettori R (1998) Effect of an obstructed ceiling on the activation time of a residential sprinkler. NISTIR 6253, National Institute of Standards and Technology, Gaithersburg
32. Vettori R (2003) Effect of a beamed, sloped, and sloped beamed ceilings on the activation time of a residential sprinkler. NISTIR 7079, National Institute of Standards and Technology, Gaithersburg
33. Hostikka S, Kokkala M, Vaari J (2001) Experimental study of the localized room fires. VTT Research Notes 2104, VTT Technical Research Centre of Finland, Espoo
34. Hamins A, Maranghides A, McGrattan K, Johnsson E, Ohlemiller T, Donnelly M, Yang J, Mulholland G, Prasad K, Kukuck S, Anleitner R, McAllister T (2005) Federal building and fire safety investigation of the world trade center disaster: experiments and modeling of structural steel elements exposed to fire. NIST NCSTAR 1–5B, National Institute of Standards and Technology, Gaithersburg
35. Peacock R, Reneke P, Davis W, Jones W (1999) Quantifying fire model evaluation using functional analysis. Fire Saf. J 33:167
36. McGrattan K, Toman B (2011) Quantifying the predictive uncertainty of complex numerical models. Metrologia 48:173